NOAA Technical Memorandum GLERL-118

CLIMATE-CORRECTED STORM-FREQUENCY EXAMPLES

Thomas E. Croley II

NOAA, Great Lakes Environmental Research Laboratory, Ann Arbor, MI 48105

Great Lakes Environmental Research Laboratory
Ann Arbor, Michigan
August 2000

UNITED STATES
DEPARTMENT OF COMMERCE

Norman Y. Mineta
Secretary

NATIONAL OCEANIC AND
ATMOSPHERIC ADMINISTRATION

D. James Baker
Under Secretary for Oceans
and Atmosphere/Administrator

NOTICE

Mention of a commercial company or product does not constitute an endorsement by the NOAA Environmental Research Laboratories. Use of information from this publication concerning proprietary products or the tests of such products for publicity or advertising purposes is not authorized. This is GLERL Contribution No. 1174.

This publication is available as a PDF file and can be downloaded from GLERL's web site: www.glerl.noaa.gov. Hard copies can be requested from the GLERL Publications Unit, 2205 Commonwealth Blvd., Ann Arbor, MI 48105. pubs.glerl@noaa.gov.

Table of Contents

Abstract 5
1. Introduction 5
2. Storm Frequency Estimation 5
3. Example Storm Frequencies 6
4. Matching Probability Forecasts 9
5. Optimum Solution 11
6. NOAA and EC Forecast Example 11
7. ENSO Conditional Forecast Example 20
8. Multiple Solutions 25
9. Summary and Observations 25
10. References 26

Figures

Figure 1.--Annual Maximum (Calendar Year) Daily Maumee River Flow Exceedance Frequency, made in September 1999 for September 1999—August 2000 (35.31 cfs = 1 m^3s^{-1}) 8

Figure 2.--Annual Maximum (Water Year) Daily Maumee River Flow Exceedance Frequency, made in September 1999 for September 1999—August 2000 (35.31 cfs = 1 m^3s^{-1}) 8

Figure 3.--NOAA Outlook of Meteorology Event Probabilities for October-November-December 1999, made 16 September 1999 12

Figure 4.--EC Outlook of Most-Probable Meteorology Event for September-October-November 1999, made 1 September 1999 13

Figure 5.--Mixed NOAA and EC Meteorology Probability Forecasts made in September 1999 over the Maumee River Basin 14

Figure 6.--Alternate Representation of (24), (11), and Equations in Figure 5 as (20) 19

Figure 7.--ENSO Event Conditional Probability Forecast Equations for Maumee River Basin 22

Figure 8.--Alternate Equations Set for La Nina and El Nino Examples as in (20) 23

Figure 9.--ENSO Annual Maximum (Calendar Year) Daily Maumee River Flow Exceedance 24

Figure 10.--ENSO Annual Maximum Daily Maumee River Basin Precipitation Exceedance 24

Tables

Table 1.--Annual Daily Maxima for the Maumee River Basin (35.31 cfs = 1 m^3s^{-1}) 7

Table 2.--Average Air Temperature over the Maumee River Basin (^oC) 16

Table 3.--Average Daily Precipitation on the Maumee River Basin (mm) 17

Table 4.--Historical Reference Quantiles of Average Air Temperature over the Maumee River Basin (^oC) 18

Table 5.--Historical Reference Quantiles of Average Daily Precipitation on the Maumee River Basin (mm) 18

Table 6.--El Nino and La Nina event onset years 21

CLIMATE-CORRECTED STORM-FREQUENCY EXAMPLES[1]

Thomas E. Croley II

ABSTRACT. Storm frequency estimates (e.g., maximum precipitation or flow probabilities) allow engineers and hydrologists to assess risks associated with their decisions during the design, construction, and operation of water resource projects. Storm frequencies for the future are often estimated directly from past historical records of sufficient length. The estimation requires no detailed knowledge of the area's meteorology, but presumes it remains unchanged in the future. However, the climate seldom remains static. Numerous climate forecasts of meteorology probabilities over extended periods are now available to the water resource engineer and hydrologist. It is possible to use these meteorology forecasts directly in the estimation of storm frequencies from the historical record. It is more desirable to do so now than at any time past, since meteorology forecasts have been improving and are now better than their predecessors. A heuristic approach is defined here to estimate storm frequencies that recognize forecasts of extended weather probabilities. Basically, those groups of historical meteorology record segments matching forecast meteorology probabilities are weighted more than others, during the estimation of storm frequencies. (Affiliated groups of hydrology record segments may be similarly weighted for hydrological estimation; e.g., flood frequency estimation.) Examples include frequency estimation of maximum daily precipitation and maximum flow, using currently available agency meteorological forecasts in the US and Canada as well as El Niño and La Niña conditional probabilities.

1. INTRODUCTION

The purpose of this report is to present application examples for modifying storm frequency estimates to reflect outside probability information that might be available, such as meteorology probability forecasts or El Niño—Southern Oscillation (El Niño and La Niña) expectations. The report consists of a brief overview of storm frequency estimation and a brief discussion of the application of techniques to alter this estimation for meteorology probability forecasts. Details of the theory and discussion of the techniques presented here are available elsewhere (Croley 1996, 1997a,b, 2000a,b). This report details the application examples omitted in the theoretical description presented by Croley (2000b).

2. STORM FREQUENCY ESTIMATION

Since storm frequencies are unknown, they are *estimated* from the historical record, which is assumed ergodic and treated as a "random sample." Successive observations are considered identically distributed and equally likely to occur (both in the past and future). Likewise, the observations must be defined so they can be considered as independent of each other. (Two successive

---

[1] GLERL Contribution No. 1174

storms occurring very closely may result in a high degree of dependence of the second on the first.) Defining long event inter-arrival times or record pieces can minimize temporal dependence. For example, annual maximum floods or rainfalls (inter-arrival time on the order of a year) are often taken as time independent, as are 1-year record segments.

Storm frequencies or "exceedance probabilities," $P[X \geq x]$ can be estimated directly from the historical record. Suppose all values, x_i, in a random sample of annual maximums (x_i, $i = 1, ..., n$) are ordered from largest to smallest to define the ordered variable values (y_ℓ, $\ell = 1, ..., n$), where $y_\ell = x_{i(\ell)}$ and $i(\ell)$ is the number of the value in the unordered sample corresponding to the $\ell^{\underline{\text{th}}}$ order. There are several methods to estimate exceedance probabilities from annual exceedance series (Chow 1964); without loss of generality, the popular "Weibull" method is used here as an example:

$$\hat{P}\left[X \geq y_\ell\right] = \frac{\ell}{n+1} = \frac{1}{n+1}\sum_{i=1}^{\ell} 1, \qquad \ell = 1, \ldots, n \tag{1}$$

The caret, "^," denotes an estimate of the characteristic named underneath. Other methods also could be used.

This estimator is called "non-parametric" since knowledge of the underlying distribution and its parameters is not required. Other estimators (called "parametric") derive from knowledge (or supposition) of the type of underlying distribution. Functions of a random sample may be used as estimators of the parameters of the underlying distribution. Several of interest here are the "sample mean," $\hat{\mu}$, "sample variance," $\hat{\sigma}^2$, and "sample skew coefficient," $\hat{\psi}$:

$$\hat{\mu} = \frac{1}{n}\sum_{i=1}^{n} x_i \tag{2}$$

$$\hat{\sigma}^2 = \frac{1}{n-1}\sum_{i=1}^{n}\left(x_i - \hat{\mu}\right)^2 \tag{3}$$

$$\hat{\psi} = \frac{n}{(n-1)(n-2)}\sum_{i=1}^{n}\left(x_i - \hat{\mu}\right)^3 \Big/ \left(\sqrt{\hat{\sigma}^2}\right)^3 \tag{4}$$

They are estimators of distribution mean, μ, variance, σ^2, and skew coefficient, ψ, respectively. Other estimators (Koutrouvelis and Canavos 1999) also could be used with no loss of generality.

3. EXAMPLE STORM FREQUENCIES

Daily precipitation data from 32 stations were assembled over 1948-1995 for the Maumee River basin, defined at its outflow point into Lake Erie with an area of 16,806 km^2. (Widespread meteorological observations began in 1948.) The annual maximum of the areal-average (Thiessen-weighted) daily basin precipitation for this data set is given in columns 2 and 6 of Table 1. Additionally, daily flow records of the Maumee River at Waterville, Ohio (basin area = 16,394.7 km^2) were searched for this period, and the annual maximum daily flows are given also in Table 1.

Table 1. Annual Daily Maxima for the Maumee River Basin (35.31 cfs = 1 m^3s^{-1}).

Year	Calendar Year		Water Year[c]	Year	Calendar Year		Water Year[c]
	Precip.[a] (mm)	Flow[b] (cfs)	Flow[b] (cfs)		Precip.[a] (mm)	Flow[b] (cfs)	Flow[b] (cfs)
(1)	(2)	(3)	(4)	(5)	(6)	(7)	(8)
1949	3.674	45100	45100	1973	2.490	40000	42800
1950	4.984	92400	92400	1974	2.295	69600	69600
1951	3.412	53100	53100	1975	2.690	49400	49400
1952	3.931	53100	53100	1976	2.532	68500	68500
1953	3.010	33200	33200	1977	4.151	64000	56200
1954	3.753	23400	23400	1978	2.518	86400	86400
1955	3.563	45900	45900	1979	3.185	53400	53400
1956	4.232	42700	42700	1980	4.511	44400	44400
1957	4.661	62400	62400	1981	4.930	85400	85400
1958	3.276	29700	40300	1982	3.776	113000	113000
1959	4.274	80000	80000	1983	3.510	54200	54200
1960	2.594	44800	44800	1984	2.420	51300	51300
1961	2.614	53500	53500	1985	2.545	91100	91100
1962	2.335	45800	45800	1986	4.018	36200	36000
1963	2.795	35200	35200	1987	3.206	23500	36200
1964	2.533	46800	46800	1988	3.779	22900	23500
1965	3.259	36200	36200	1989	3.370	42700	42700
1966	3.561	79000	26200	1990	4.164	82000	62500
1967	2.592	48900	79000	1991	4.187	86700	86700
1968	3.537	56900	56900	1992	3.625	54000	36700
1969	4.511	67500	67500	1993	2.359	65000	65000
1970	3.580	33300	33300	1994	2.685	63900	63900
1971	3.785	38900	38900	1995	2.918	51000	51000
1972	5.575	46900	46900				

[a]Areal-average daily precipitation for Maumee River basin at Lake Erie, Ohio.
[b]Maumee River at Waterville, Ohio, Lat. 41:30:00, Long. 83:42:46.
[c]"Water Year" is defined by its end (e.g., water year 1949 ends 30 September 1949).

Both the calendar year of 1 January—31 December (columns 3 and 7) and the water year of 1 October—30 September (columns 4 and 8) were used to define the annual maximum daily flow. The exceedance frequencies for the annual maximum flows were estimated with (1) and plotted in Figures 1 and 2 as "non-parametric sans forecast."

The log-Pearson Type III distribution also was fit to the data sets of Table 1. This distribution results from supposing the natural logarithms of the data in Table 1 [$Z = \ln(X)$] are distributed as a three-parameter gamma distribution:

$$f_Z(z) = \frac{1}{|\beta|\,\Gamma(\alpha)}\left[\frac{z-c}{\beta}\right]^{\alpha-1} e^{-\frac{z-c}{\beta}}, \qquad c \le z < \infty \quad (\beta > 0) \qquad -\infty < z \le c \quad (\beta < 0) \tag{5}$$

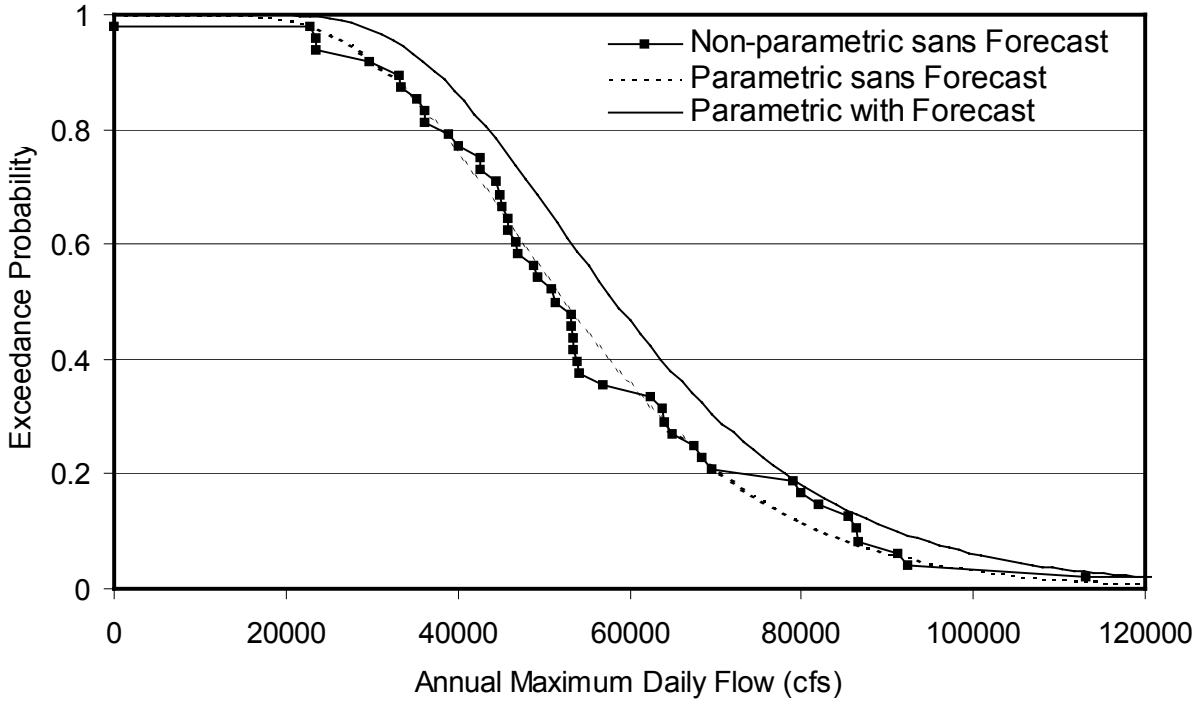

Figure 1. Annual Maximum (Calendar Year) Daily Maumee River Flow Exceedance Frequency, made in September 1999 for September 1999—August 2000 (35.31 cfs = 1 m^3s^{-1}).

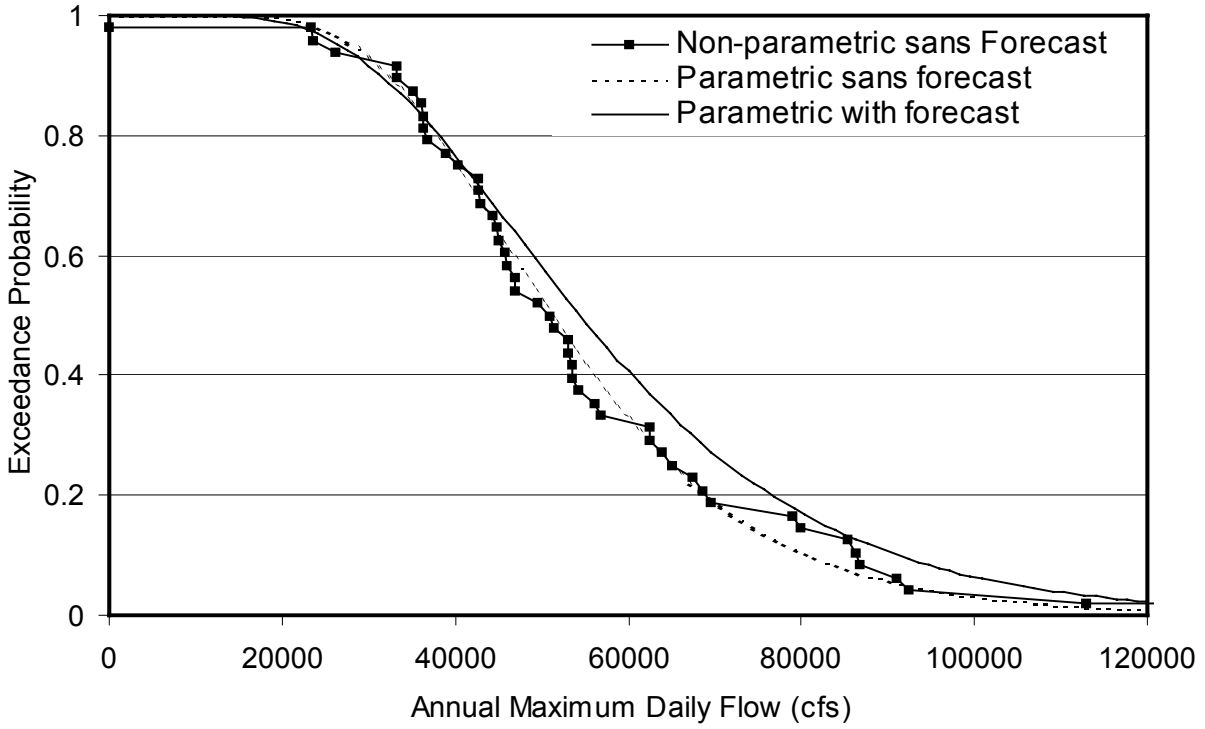

Figure 2. Annual Maximum (Water Year) Daily Maumee River Flow Exceedance Frequency, made in September 1999 for September 1999—August 2000 (35.31 cfs = 1 m^3s^{-1}).

where $f_Z(z) = \frac{\partial}{\partial z} P[Z \le z]$, $\Gamma(\alpha)$ is the gamma function, and $\alpha, \beta,$ and c are distribution parameters. Parameter estimates are given in terms of (2)—(4) defined on the natural logarithms of the data (USWRC 1967) by replacing expected values from (5) with sample moments:

$$\hat{\alpha} = (2/\hat{\psi})^2 \tag{6}$$

$$\hat{\beta} = \sqrt{\hat{\sigma}^2}\,\hat{\psi}/2 \tag{7}$$

$$\hat{c} = \hat{\mu} - 2\sqrt{\hat{\sigma}^2}/\hat{\psi} \tag{8}$$

The estimated log-Pearson Type III distributions are shown also in Figures 1 and 2 as "parametric sans forecast." See Koutrouvelis and Canavos (1999) for other parameter estimators.

4. MATCHING PROBABILITY FORECASTS

The probability of any event A, $P[\mathrm{A}]$, can be inferred with the estimator, $\hat{P}[\mathrm{A}]$, defined as the number of observations in the random sample for which A occurs (i.e., for which the event A is true), n_{A}, divided by the total number of observations in the sample, n:

$$\hat{P}[\mathrm{A}] = \frac{n_{\mathrm{A}}}{n} = \frac{1}{n}\sum_{i|\mathrm{A}} 1 \tag{9}$$

In (9), the sum is taken over all i (members of the random sample) for which A occurs, denoted as $i|\mathrm{A}$. The estimate in (9) is seen as the "relative frequency" of A in the random sample. Croley (1996, 1997a,b, 2000a,b) *biased* samples, by multiplying observations by non-negative weights, w_i, to calculate probabilities matching others' *multiple* probability forecasts:

$$\hat{P}[\mathrm{A}] = \frac{1}{n}\sum_{i|\mathrm{A}} w_i \tag{10}$$

$$\sum_{i=1}^{n} w_i = n \tag{11}$$

Consider, for example, that others' forecasts of event probability can be interpreted in $m-1$ probability equations (Croley 1996) and forecasts of most-probable events can be interpreted in u probability inequalities (Croley 2000a). They are expressed in terms of relative frequencies over a random sample as follows:

$$\begin{aligned} \hat{P}[\mathrm{A}_k] &= a_k, \qquad k = 2,\ldots,m \\ \hat{P}[\mathrm{A}_k] &\le a_k, \qquad k = m+1,\ldots,m+u \end{aligned} \tag{12}$$

where a_k are the forecast probabilities. Equation (10), when applied to match the forecasts of meteorology probabilities in (12) and added to (11), yield a system of equations to be solved for the weights:

$$
\begin{aligned}
\sum_{i=1}^{n} w_i &= n \\
\sum_{i|\mathrm{A}_k} w_i &= n\, a_k, \qquad k = 2, \ldots, m \\
\sum_{i|\mathrm{A}_k} w_i &\le n\, a_k, \qquad k = m+1, \ldots, m+u
\end{aligned}
\tag{13}
$$

Equivalently,

$$
\begin{aligned}
\sum_{i=1}^{n} \alpha_{k,i} w_i &= e_k, \qquad k = 1, \ldots, m \\
\sum_{i=1}^{n} \alpha_{k,i} w_i &\le e_k, \qquad k = m+1, \ldots, m+u
\end{aligned}
\tag{14}
$$

where $\alpha_{k,i} = 1$ for $k = 1$ or for $k > 1$ and $i \,|\, \mathrm{A}_k$ [inclusion of the $i^{\underline{\text{th}}}$ random sample value ($i^{\underline{\text{th}}}$ event or segment of the historical record) in the event of the $k^{\underline{\text{th}}}$ probability statement]; otherwise it is zero. Also, $e_k = n$ for $k = 1$ and $e_k = n\, a_k$ for $k > 1$. Any weights that satisfy (14) yield weighted-sample relative frequencies of events that match forecasts of meteorology probabilities. These weights also yield other corresponding biased sample estimators; e.g., (1)—(4) become:

$$
\hat{P}\left[X > y_\ell\right] = \frac{1}{n+1} \sum_{k=1}^{\ell} w_{i(k)}, \qquad \ell = 1, \ldots, n \tag{15}
$$

$$
\hat{\mu} = \frac{1}{n} \sum_{i=1}^{n} w_i\, x_i \tag{16}
$$

$$
\hat{\sigma}^2 = \frac{1}{n-1} \sum_{i=1}^{n} w_i \left(x_i - \hat{\mu}\right)^2 \tag{17}
$$

$$
\hat{\psi} = \frac{n}{(n-1)(n-2)} \sum_{i=1}^{n} w_i \left(x_i - \hat{\mu}\right)^3 \Big/ \left(\sqrt{\hat{\sigma}^2}\right)^3 \tag{18}
$$

Generally, some of the equations in (13) or (14) may be either redundant or infeasible (non-intersecting with the rest, resulting in no solutions) and must be eliminated. (If the number of equations is greater than the number of weights, then some of the equations *must be* either redundant or infeasible.) In practice, one could assign each equation in (13) or (14) a "priority" reflecting its importance. [The highest priority is given to the first equation in (13) or (14) corresponding to (11), guaranteeing that all relative-frequencies sum to unity.] Each equation (starting with the second highest priority equation) is compared to the set of all higher-priority equations and eliminated if redundant or infeasible. Thus (14) can always be reduced so that the allowed number of forecasts of meteorology probabilities is less than or equal to the number of historical record pieces (sample size). If less, then there are multiple solutions to (14), and a choice must be made as to which solution to use.

5. OPTIMUM SOLUTION

If there are multiple solutions to (14), the identification of the "best" requires a *measure* or *objective function* for comparing them. Solutions of (14) with larger values of this measure can be judged "better" than those with smaller values. One such measure is the probability of a selected event. If the objective function is always a statement of maximizing or minimizing a *probability*, then it can be added to the problem statement of (14) to yield an optimization problem. Objective functions that use probability statements can be expressed in the general form:

$$\max \sum_{i=1}^{n} \alpha_{0,i} w_i \tag{19}$$

where $\alpha_{0,i}$ are defined similarly to (14) in which the objective function is equation 0. The problem of solving (14) can now be formulated as an optimization, maximizing the objective function subject to a "constraint set" of equations:

$$\begin{aligned} &\max \sum_{i=1}^{n} \alpha_{0,i} w_i \quad \text{subject to} \\ &\sum_{i=1}^{n} \alpha_{k,i} w_i = e_k, \qquad k = 1, \ldots, m \\ &\sum_{i=1}^{n} \alpha_{k,i} w_i \le e_k, \qquad k = m+1, \ldots, m+u \\ &w_i \ge 0, \qquad i = 1, \ldots, n \end{aligned} \tag{20}$$

Equations (20) are amenable to standard "linear programming" optimization techniques. An algebraic procedure, termed the "Simplex" method, has been developed (Hillier and Lieberman 1969) which progressively approaches the optimum solution through a well-defined iterative process until optimality is finally reached. Croley (2000a,b) describes a procedure for applying the Simplex method in a two-stage optimization. The first stage finds a feasible solution to the constraint set in (20) and the second searches systematically from that feasible solution to the optimum solution. Multiple optima are possible, depending upon the objective function and the constraint set.

6. NOAA AND EC FORECAST EXAMPLE

The estimates of Figure 1 are modified by incorporating selected forecasts from the National Oceanic and Atmospheric Administration (NOAA event probability forecasts) and Environment Canada (EC most-probable event forecasts); see Croley (1996, 1997b, 2000a). An example for NOAA is given in Figure 3. The NOAA outlook estimates probabilities of average air temperature and total precipitation falling within pre-selected value ranges. The value ranges (low, normal, and high) are defined as the lower, middle, and upper thirds of observations over period 1961—90 for each variable. The climate outlooks presume that one of only four possibilities exists for the probability distribution type for each variable: 1) the probability of being in the high range exceeds one-third, and the probability of being in the low range is reduced accordingly (it

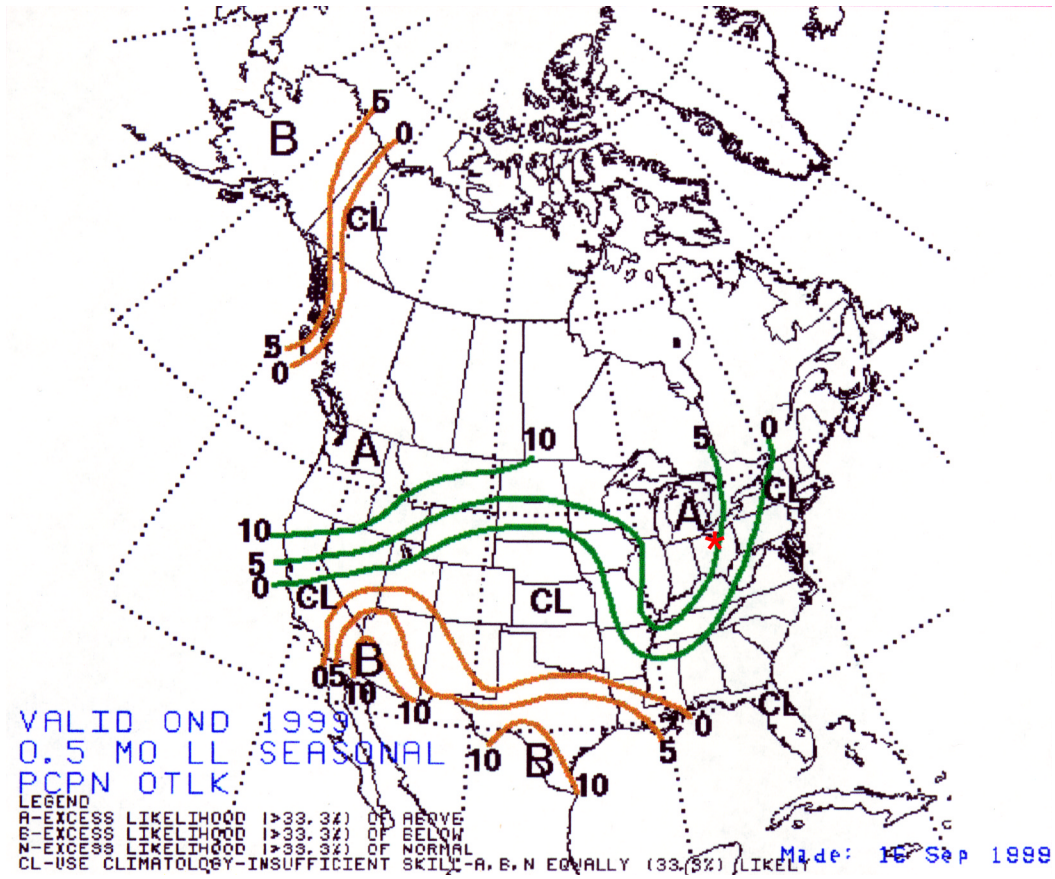

Figure 3. NOAA Outlook of Meteorology Event Probabilities for October-November-December 1999, made 16 September 1999.

remains at one-third for the normal range)—referred to as being "above normal"; 2) the probability of being in the normal range exceeds one-third, and the probabilities of being in the low and high ranges are reduced accordingly and are equal—referred to as being "normal"; 3) the probability of being in the low range exceeds one-third, and the probability of being in the high range is reduced accordingly (it remains at one-third for the normal range)—referred to as being "below normal"; or 4) skill is insufficient to make a forecast, and so probabilities of one-third in each range are used—referred to "climatological." From Figure 3 at the Maumee River basin (near the southwest edge of Lake Erie, marked by a red asterisk), the probability of October-November-December (OND) total precipitation in the upper third of historical observations is forecast to rise by about 0.05. According to the convention of NOAA's definitions then, the corresponding probability of OND precipitation in the lower third of historical observations is forecast to drop by about 0.05, and the probability of OND precipitation in the middle third of historical observations is forecast to remain unchanged at one-third:

$$
\begin{aligned}
\hat{P}\left[Q_{OND99} \le \hat{\theta}_{OND,0.333}\right] &= 0.333 - 0.05 = 0.283 \\
\hat{P}\left[\hat{\theta}_{OND,0.333} < Q_{OND99} \le \hat{\theta}_{OND,0.667}\right] &= 0.334 \\
\hat{P}\left[Q_{OND99} > \hat{\theta}_{OND,0.667}\right] &= 0.333 + 0.05 = 0.383
\end{aligned}
\tag{21}
$$

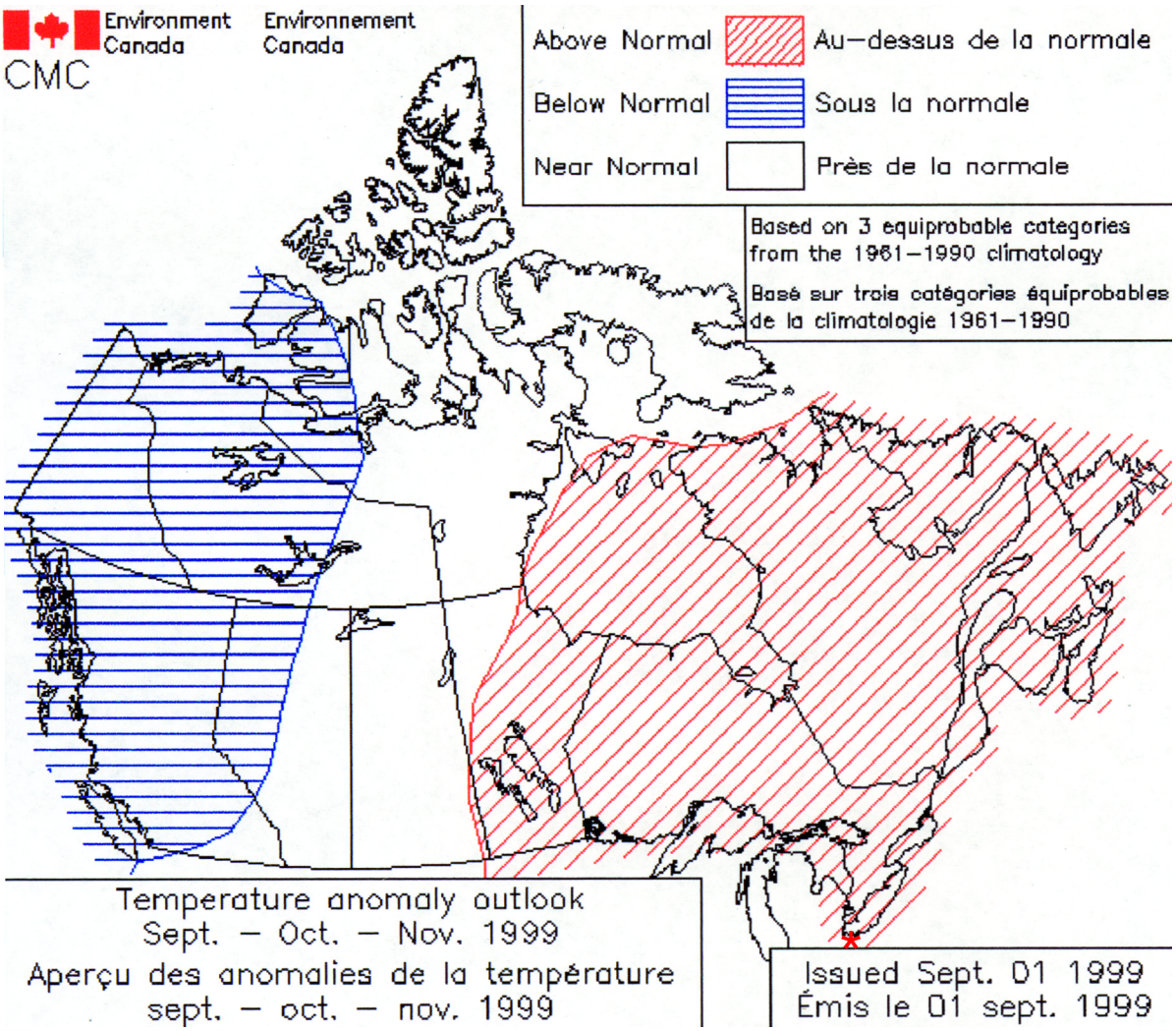

Figure 4. EC Outlook of Most-Probable Meteorology Event for September-October-November 1999, made 1 September 1999.

where Q_g = total precipitation for period g and $\hat{\theta}_{g,\gamma}$ is the γ-quantile for period g precipitation estimated from a reference historical period (1961—90) such that:

$$\hat{P}\left[Q_g \le \hat{\theta}_{g,\gamma}\right] = \gamma \tag{22}$$

Likewise, air temperature, T_g, and its quantiles, $\hat{\tau}_{g,\gamma}$, are defined similarly to (22). Noting that the second line of (21) is redundant with the rest of (21) and the fact that all probabilities must sum to unity, we need only keep the top and bottom lines in (21).

An example for EC is given in Figure 4. The EC outlook indicates which of three pre-selected ranges of values (lower, middle, or upper thirds of observations from 1961—90 for precipitation or from 1963—93 for temperature) are most likely to occur for 1- and 3-month air temperature and 1- and 3-month total precipitation. Figure 4 at the Maumee River basin (marked with a red

$$\hat{P}\left[Q_{OND'99} \le \hat{\theta}_{OND,0.333}\right] = 0.283 \quad (1)$$
$$\hat{P}\left[Q_{OND'99} > \hat{\theta}_{OND,0.667}\right] = 0.383 \quad (2)$$
$$\hat{P}\left[Q_{NDJ'99} \le \hat{\theta}_{NDJ,0.333}\right] = 0.273 \quad (3)$$
$$\hat{P}\left[Q_{NDJ'99} > \hat{\theta}_{NDJ,0.667}\right] = 0.393 \quad (4)$$
$$\hat{P}\left[Q_{DJF'99} \le \hat{\theta}_{DJF,0.333}\right] = 0.273 \quad (5)$$
$$\hat{P}\left[Q_{DJF'99} > \hat{\theta}_{DJF,0.667}\right] = 0.393 \quad (6)$$
$$\hat{P}\left[Q_{JFM'00} \le \hat{\theta}_{JFM,0.333}\right] = 0.133 \quad (7)$$
$$\hat{P}\left[Q_{JFM'00} > \hat{\theta}_{JFM,0.667}\right] = 0.533 \quad (8)$$
$$\hat{P}\left[Q_{FMA'00} \le \hat{\theta}_{FMA,0.333}\right] = 0.273 \quad (9)$$
$$\hat{P}\left[Q_{FMA'00} > \hat{\theta}_{FMA,0.667}\right] = 0.393 \quad (10)$$
$$\hat{P}\left[Q_{MAM'00} \le \hat{\theta}_{MAM,0.333}\right] = 0.273 \quad (11)$$
$$\hat{P}\left[Q_{MAM'00} > \hat{\theta}_{MAM,0.667}\right] = 0.393 \quad (12)$$
$$\hat{P}\left[T_{OND'99} \le \hat{\tau}_{OND,0.333}\right] = 0.333 \quad (13)$$
$$\hat{P}\left[T_{OND'99} > \hat{\tau}_{OND,0.667}\right] = 0.333 \quad (14)$$
$$\hat{P}\left[T_{NDJ'99} \le \hat{\tau}_{NDJ,0.333}\right] = 0.333 \quad (15)$$
$$\hat{P}\left[T_{NDJ'99} > \hat{\tau}_{NDJ,0.667}\right] = 0.333 \quad (16)$$
$$\hat{P}\left[T_{DJF'99} \le \hat{\tau}_{DJF,0.333}\right] = 0.273 \quad (17)$$
$$\hat{P}\left[T_{DJF'99} > \hat{\tau}_{DJF,0.667}\right] = 0.393 \quad (18)$$
$$\hat{P}\left[T_{JFM'00} \le \hat{\tau}_{JFM,0.333}\right] = 0.263 \quad (19)$$
$$\hat{P}\left[T_{JFM'00} > \hat{\tau}_{JFM,0.667}\right] = 0.403 \quad (20)$$
$$\hat{P}\left[T_{FMA'00} \le \hat{\tau}_{FMA,0.333}\right] = 0.333 \quad (21)$$
$$\hat{P}\left[T_{FMA'00} > \hat{\tau}_{FMA,0.667}\right] = 0.333 \quad (22)$$
$$\hat{P}\left[T_{MAM'00} \le \hat{\tau}_{MAM,0.333}\right] = 0.333 \quad (23)$$
$$\hat{P}\left[T_{MAM'00} > \hat{\tau}_{MAM,0.667}\right] = 0.333 \quad (24)$$
$$\hat{P}\left[Q_{SON'99} \le \hat{\theta}_{SON,0.333}\right] \le 0.333 \quad (25)$$
$$\hat{P}\left[\hat{\theta}_{SON,0.333} < Q_{SON'99} \le \hat{\theta}_{SON,0.667}\right] \ge 0.334 \quad (26)$$
$$\hat{P}\left[Q_{SON'99} > \hat{\theta}_{SON,0.667}\right] \le 0.333 \quad (27)$$
$$\hat{P}\left[Q_{JJA'00} \le \hat{\theta}_{JJA,0.333}\right] \le 0.333 \quad (28)$$
$$\hat{P}\left[\hat{\theta}_{JJA,0.333} < Q_{JJA'00} \le \hat{\theta}_{JJA,0.667}\right] \le 0.334 \quad (29)$$
$$\hat{P}\left[Q_{JJA'00} > \hat{\theta}_{JJA,0.667}\right] \ge 0.333 \quad (30)$$
$$\hat{P}\left[T_{SON'99} \le \hat{\tau}_{SON,0.333}\right] \le 0.333 \quad (31)$$
$$\hat{P}\left[\hat{\tau}_{SON,0.333} < T_{SON'99} \le \hat{\tau}_{SON,0.667}\right] \le 0.334 \quad (32)$$
$$\hat{P}\left[T_{SON'99} > \hat{\tau}_{SON,0.667}\right] \ge 0.333 \quad (33)$$
$$\hat{P}\left[T_{DJF'99} \le \hat{\tau}_{DJF,0.333}\right] \le 0.333 \quad (34)$$
$$\hat{P}\left[\hat{\tau}_{DJF,0.333} < T_{DJF'99} \le \hat{\tau}_{DJF,0.667}\right] \le 0.334 \quad (35)$$
$$\hat{P}\left[T_{DJF'99} > \hat{\tau}_{DJF,0.667}\right] \ge 0.333 \quad (36)$$
$$\hat{P}\left[T_{JJA'00} \le \hat{\tau}_{JJA,0.333}\right] \ge 0.333 \quad (37)$$
$$\hat{P}\left[\hat{\tau}_{JJA,0.333} < T_{JJA'00} \le \hat{\tau}_{JJA,0.667}\right] \le 0.334 \quad (38)$$
$$\hat{P}\left[T_{JJA'00} > \hat{\tau}_{JJA,0.667}\right] \le 0.333 \quad (39)$$

Figure 5. Mixed NOAA and EC Meteorology Probability Forecasts Made in September 1999 over the Maumee River Basin.

asterisk) shows that above-normal air temperatures are expected for the September-October-November period, which is interpreted as follows:

$$\begin{aligned} \hat{P}\left[T_{SON99} \le \hat{\tau}_{SON,0.333}\right] &\le 0.333 \\ \hat{P}\left[\hat{\tau}_{SON,0.333} < T_{SON99} \le \hat{\tau}_{SON,0.667}\right] &\le 0.333 \\ \hat{P}\left[T_{SON99} > \hat{\tau}_{SON,0.667}\right] &\ge 0.333 \end{aligned} \quad (23)$$

All 28 NOAA forecast maps, like Figure 3, which were published in September 1999, were selectively read and interpreted as in (21) and the results are summarized in Figure 5 as equations 1 through 24. All eight EC forecast maps, like Figure 4, which were available in September 1999, were also selectively read and interpreted as in (23) and the results are summarized in Figure 5 as equations 25 through 39. The forecasts summarized in Figure 5 are in priority order with the ear-

liest-made forecasts first (NOAA equalities precede EC inequalities), precipitation before temperature second, and chronologically third.

Note that the precipitation forecasts in Figure 5 are for high precipitation with only one exception (the EC SON forecast). The objective in matching these forecasts is therefore (arbitrarily) taken as maximizing the probability that precipitation over the period November 1999—July 2000 will be in the upper third of its historical range (determined from 1961—1990):

$$\max \hat{P}\left[Q_{Nov'99-Jul'00} > \hat{\theta}_{Nov-Jul,\,0.667} \right] \tag{24}$$

Daily precipitation and air temperature data from 32 stations were assembled over 1948-1995 for the Maumee River basin. (Widespread meteorology observations began in 1948.) The data were used to determine the Thiessen-averaged air temperature and the total precipitation, for the periods shown in Figure 5 and (24), which are given in Tables 2 and 3. According to the agencies, the NOAA temperature and precipitation forecasts and the EC precipitation forecasts are defined relative to historical reference quantiles estimated over the 1961-1990 period. Likewise, the EC temperature forecasts are defined relative to historical reference quantiles estimated over the 1963-1993 period. By ordering data from these periods, the reference quantiles are estimated in Tables 4 and 5.

Consider the objective function of (24) and the forecasts of Figure 5 to apply prior to and through the *beginning* of each year in the sample, so that the time lag accounts for meteorology driving hydrology. (The Maumee River annual maximum flow typically occurs as spring snowmelt.) In other words, each year of record is to be weighted to reflect the objective of (24) and the beginning winter as forecast in Figure 2 (a total period from September of the year before through the following August). For example, the first value in Table 1 for calendar year 1949 corresponds to the objective and forecast values for September 1948—August 1949. The coefficients in (20) are derived from the data set, Figure 2, and (24); see Croley (2000a). In the ensuing optimization, 19 weights are zeroes, indicating that some of the historical record is not used. However, all but the last three equations in Figure 2 are used (corresponding to all forecasts except the EC most-probable JJA air temperature forecast).

Suppose now that a hydrologist has acquired, in September 1999, the forecasts of Figure 5 and wishes to make an estimate of storm frequencies (annual maximum Maumee River flows) at that time for the coming winter and following spring and summer (September 1999—August 2000). He or she would consider each of the possibilities in Table 1 as a possibility for this period. (The Maumee River annual maximum flow typically occurs as spring snowmelt.) The objective function of (24) and the forecasts of Figure 5 would apply prior and through the *beginning* of each year in the sample, so that the time lag accounts for the meteorology driving the hydrology. In other words, each year of record is to be weighted to reflect the objective of (24) and the beginning winter as forecast in Figure 5 (a total period from September of the year before through the following August). For example, the first value in Table 1 for calendar year 1949 corresponds to the objective and forecast values for September 1948—August 1949. The coefficients in (20), $\alpha_{k,i}$, have values of 1 or 0 corresponding to the inclusion or exclusion, respectively, of each variable in the sets indicated in the variable subscripts in (24) and Figure 5. For (24), the reader

Table 2. Average Air Temperature over the Maumee River Basin (ºC).

	Start in Year					Start in Following Year			
Year (1)	SON (2)	OND (3)	NDJ (4)	Nov-Apr (5)	DJF (6)	JFM (7)	FMA (8)	MAM (9)	JJA (10)
1948	12.28	5.93	2.76	3.69	0.40	1.66	4.64	9.95	23.21
1949	11.35	6.63	2.30	1.99	0.09	0.10	1.67	7.82	20.70
1950	11.04	3.55	-1.74	0.80	-3.06	-0.26	3.39	9.47	21.17
1951	10.49	4.12	-0.54	1.82	-0.94	0.67	4.23	9.03	23.24
1952	10.99	5.26	2.08	3.22	0.27	1.60	4.38	9.87	23.12
1953	12.69	6.81	1.61	3.64	0.26	0.73	5.72	9.33	22.08
1954	12.22	5.47	0.13	2.67	-1.85	-0.36	5.27	11.21	23.02
1955	11.50	4.18	-1.38	0.75	-2.80	-1.16	2.93	8.38	21.88
1956	12.08	7.17	0.20	2.41	-1.34	-0.88	4.67	9.61	21.89
1957	10.82	5.42	1.00	1.78	-2.20	-1.94	2.58	9.28	20.57
1958	12.01	4.10	-1.90	0.81	-4.52	-1.59	3.59	10.35	23.02
1959	11.21	5.15	0.75	1.23	-0.81	-2.59	1.73	7.30	21.17
1960	12.50	4.42	-1.35	1.40	-3.11	0.09	4.21	8.53	21.29
1961	12.72	5.02	-1.11	0.80	-3.96	-2.41	2.76	10.30	21.49
1962	11.20	4.18	-2.96	-0.22	-6.56	-3.49	2.58	9.55	21.07
1963	13.40	5.50	-0.44	1.45	-3.69	-0.58	3.39	10.22	21.84
1964	11.46	4.82	0.33	1.00	-2.77	-2.50	1.69	8.88	20.58
1965	11.76	6.22	0.57	1.99	-1.89	-1.20	3.45	8.16	21.97
1966	10.39	4.40	0.64	1.84	-2.63	-0.91	3.08	8.74	20.88
1967	9.77	4.51	-1.22	1.14	-3.31	-1.89	3.55	9.38	21.94
1968	11.74	4.97	-0.70	1.26	-3.11	-2.00	3.26	9.25	21.26
1969	10.50	3.63	-2.98	-0.15	-4.94	-3.64	2.73	9.46	21.74
1970	12.10	5.49	-0.97	0.72	-3.20	-2.60	2.45	7.97	21.65
1971	13.25	7.41	0.69	1.42	-1.96	-2.09	2.17	8.81	20.58
1972	10.09	3.75	0.09	2.46	-1.81	1.08	4.89	10.14	22.40
1973	13.01	5.95	0.26	1.95	-2.85	-0.89	3.68	9.42	21.40
1974	10.40	4.70	0.74	1.30	-1.67	-0.74	1.87	8.52	21.96
1975	11.53	6.21	0.17	2.98	-1.98	0.29	5.85	10.03	21.08
1976	8.22	0.94	-5.94	-0.52	-7.41	-3.35	5.02	12.58	21.39
1977	11.19	3.77	-2.40	-1.65	-7.55	-6.56	-0.90	7.74	21.31
1978	11.82	4.78	-1.26	0.02	-5.88	-4.05	1.32	9.24	20.96
1979	11.22	5.48	0.47	0.76	-3.10	-3.04	1.05	8.27	22.06
1980	10.47	3.50	-1.96	1.07	-3.65	-1.76	4.17	9.22	21.64
1981	10.34	3.91	-2.20	-0.58	-5.68	-4.16	1.08	9.31	20.75
1982	11.73	7.16	2.33	3.24	0.51	0.84	4.18	8.52	23.24
1983	12.12	3.69	-2.96	-0.27	-4.64	-3.06	2.47	6.53	22.05
1984	11.66	6.72	-0.14	2.22	-3.05	-2.04	4.63	11.79	20.71
1985	12.50	4.45	-0.89	1.61	-4.19	-0.62	4.16	10.75	21.25
1986	11.57	5.04	-0.28	2.33	-1.46	0.21	5.00	11.13	22.74
1987	11.06	5.19	0.78	1.68	-2.88	-2.11	2.60	9.73	23.51
1988	10.21	3.71	1.16	1.75	-1.94	-0.26	2.36	8.47	21.53
1989	10.50	2.11	-1.35	1.82	-2.48	2.27	5.05	9.52	21.07
1990	12.00	6.13	1.04	3.15	-1.33	0.08	5.30	11.90	22.73
1991	10.96	5.35	0.30	2.09	-0.48	0.36	3.92	8.62	19.72
1992	10.55	4.80	0.75	1.22	-2.29	-1.83	1.71	8.49	22.16
1993	10.06	4.22	-2.00	0.37	-4.98	-3.49	2.80	9.14	21.40
1994	12.35	6.84	1.67	2.30	-1.83	-0.77	2.95	9.06	23.31

Table 3. Average Daily Precipitation on the Maumee River Basin (mm).

	Start in Year					Start in Following Year			
Year (1)	SON (2)	OND (3)	NDJ (4)	Nov-July (5)	DJF (6)	JFM (7)	FMA (8)	MAM (9)	JJA (10)
1948	2.56	2.52	3.19	2.88	2.74	2.53	2.04	2.52	3.02
1949	2.03	2.03	3.27	3.24	4.42	4.47	3.65	2.59	3.80
1950	3.66	2.87	2.40	2.91	2.04	2.31	2.89	3.00	2.95
1951	2.33	2.86	3.03	2.82	2.79	2.71	2.68	3.46	1.98
1952	1.71	1.49	1.91	2.15	1.62	2.13	2.13	2.61	2.17
1953	1.02	0.96	1.40	2.29	1.97	2.42	2.72	2.67	3.37
1954	2.81	2.90	1.58	2.15	1.72	2.20	2.47	2.31	2.76
1955	3.02	2.61	1.64	2.49	1.23	2.03	2.64	3.33	2.81
1956	0.81	1.31	1.71	2.60	1.70	1.39	2.66	3.32	2.76
1957	2.79	2.84	2.11	2.53	1.71	0.78	1.15	1.68	4.62
1958	2.38	1.50	2.30	2.67	2.12	2.86	3.06	3.05	2.48
1959	2.99	2.74	2.40	2.34	2.24	1.77	1.51	1.85	2.64
1960	1.24	1.10	0.75	2.39	1.17	2.19	3.73	3.44	2.91
1961	2.27	1.58	1.97	1.98	1.84	1.95	1.45	1.79	2.27
1962	1.71	1.25	0.89	1.88	0.72	1.62	2.11	2.53	2.45
1963	0.87	0.86	1.27	2.24	0.98	2.03	3.15	3.46	2.27
1964	1.01	1.06	1.98	2.30	2.43	2.58	2.62	2.63	2.60
1965	2.67	2.42	1.57	2.00	1.49	1.13	1.72	2.08	2.86
1966	2.49	3.14	3.21	2.62	2.26	1.69	2.19	2.68	1.93
1967	2.52	3.38	2.91	2.81	2.48	1.49	1.67	2.97	3.05
1968	2.17	2.33	3.06	2.77	2.12	1.57	1.62	2.62	2.75
1969	2.99	2.01	1.58	2.49	0.91	1.25	2.40	3.23	2.59
1970	2.54	1.85	1.44	2.11	1.59	1.57	1.58	1.99	2.41
1971	2.16	2.13	1.91	2.48	1.71	1.36	2.49	3.30	2.80
1972	3.95	2.67	2.46	2.94	1.52	2.09	2.40	3.18	3.61
1973	1.94	2.58	2.74	2.43	2.37	2.41	2.35	2.96	1.94
1974	1.85	1.96	2.47	2.63	2.34	2.11	2.16	2.50	4.03
1975	2.08	2.10	2.18	2.51	2.32	2.53	2.55	2.48	2.47
1976	1.61	1.02	0.61	1.98	1.04	2.03	3.03	2.82	3.35
1977	2.49	2.28	2.67	2.37	2.21	1.83	2.13	2.72	2.41
1978	1.75	1.98	2.16	2.45	1.86	1.70	2.03	2.58	3.69
1979	2.06	2.46	2.16	2.71	1.38	1.80	2.41	2.83	4.05
1980	1.43	1.34	1.02	2.56	1.43	1.03	2.30	2.71	4.01
1981	2.74	2.04	2.11	2.46	2.32	2.73	2.29	2.89	2.28
1982	2.57	2.84	2.84	2.65	1.36	1.10	2.26	3.05	2.24
1983	3.41	3.81	2.77	2.62	1.65	1.45	2.60	3.45	1.90
1984	2.62	2.31	2.12	2.38	2.13	2.62	2.57	2.45	2.95
1985	3.34	3.17	2.44	3.00	1.53	1.64	2.38	2.35	4.35
1986	2.96	2.09	1.51	1.92	1.10	1.02	1.00	1.91	3.39
1987	1.76	2.27	1.98	1.71	1.81	1.39	1.68	1.43	2.21
1988	2.84	2.64	2.30	2.65	1.43	1.42	1.88	3.14	3.15
1989	2.14	1.50	1.48	2.81	2.36	2.64	2.76	2.76	3.91
1990	2.62	3.53	2.88	2.41	2.56	1.32	1.98	2.93	2.04
1991	2.69	2.55	1.52	2.51	1.19	1.63	2.24	2.68	3.80
1992	3.71	2.71	3.12	2.88	2.15	2.41	2.37	2.45	3.06
1993	2.75	1.85	2.01	2.10	1.35	1.32	2.04	2.02	2.78
1994	1.51	1.89	2.36	2.39	1.69	1.51	2.03	2.80	2.77

Table 4. Historical Reference Quantiles of Average Air Temperature over the Maumee River Basin (ºC).

Quantile	Period, i										
	SON[a]	SON[b]	OND[a]	NDJ[a]	Nov-Apr[a]	DJF[a]	DJF[b]	JFM[a]	FMA[a]	MAM[a]	JJA[b]
(1)	(2)	(3)	(4)	(5)	(6)	(7)	(8)	(9)	(10)	(11)	(12)
$\hat{\tau}_{i,\,0.333}$	10.50	10.50	4.18	-1.22	0.80	-3.69	-3.54	-2.5	2.47	8.45	21.15
$\hat{\tau}_{i,\,0.667}$	11.74	11.71	5.19	0.26	1.75	-2.63	-2.35	-0.89	3.68	9.31	21.84

[a]Quantiles based on the period: 1961-1990.
[b]Quantiles based on the period: 1963-1993.

Table 5. Historical Reference Quantiles[a] of Average Daily Precipitation on the Maumee River Basin (mm).

Quantile	Period, i								
	SON	OND	NDJ	DJF	JFM	FMA	MAM	JJA	Nov-July
(1)	(2)	(3)	(4)	(5)	(6)	(7)	(8)	(9)	(10)
$\hat{\theta}_{i,\,0.333}$	2.06	1.98	1.91	1.49	1.49	2.11	2.49	2.45	2.37
$\hat{\theta}_{i,\,0.667}$	2.57	2.42	2.44	2.13	2.03	2.40	2.83	3.01	2.62

[a]Quantiles based on the period: 1961-1990.

can see from inspection of column 5 in Table 3 that the relation, $q_{Nov-Jul} > \hat{\theta}_{Nov-Jul,\,0.667}$ (or $q_{Nov-Jul} > 2.62$ mm ; see column 10 in Table 5) is satisfied by the following indices: 1 (corresponding to 1948), 2, 3, 4, 11, 19, 20, 21, 25, 27, 32, 35, 38, 41, 42, and 45 (corresponding to 1992). [Index 19 (corresponding to 1966) does not appear to satisfy this relation because of round-off error, but in fact does.] Thus, (24) would be written, similar to the first line in (20), as

$$\max\,(w_1+w_2+w_3+w_4+w_{11}+w_{19}+w_{20}+w_{21}+w_{25}+w_{27}+w_{32}+w_{35}+w_{38}+w_{41}+w_{42}+w_{45}) \qquad (25)$$

Expressing (25) in vector form,

$$\max\,\left[1111000000100000001110001010000100100100110010 0\right]\mathbf{w} \qquad (26)$$

where **w** = the column vector of the weights. Likewise, the reader can see from inspection of Tables 2—5 that (24), (11), and Figure 5 become, similar to (20) [with (11) first in the constraint set], the vector equation set shown in Figure 6. In the ensuing optimization of Figure 6, 19 weights are zeroes, indicating that some of the historical record is not used. However, all but the last three equations in Figures 5 and 6 are used (corresponding to all forecasts except the EC most-probable JJA air temperature forecast).

Climate-*biased* storm frequencies for the annual (calendar year) maximum daily flow can now be estimated by applying these weights to the data in column 3 of Table 1 by using (15)—(18). Only results for the fitted Log-Pearson Type III distribution (to simplify the presentation) are given in Figure 1. Compare the Log-Pearson Type III distribution derived from the parametric

$$
\begin{array}{lll}
\max & [111100000010000000111000101000010010010011001 00] \, \mathbf{w} & \text{subject to} \\
 & [1111111111111111111111111111111111111111111111111] \, \mathbf{w} & = 47 \\
 & [0000110010101111100000100010101010000000100011] \, \mathbf{w} & = 0.283 \times 47 \\
 & [1011001101010000001100001100000100110100101 1100] \, \mathbf{w} & = 0.383 \times 47 \\
 & [0000011110001011010001110000100010000010010 1000] \, \mathbf{w} & = 0.273 \times 47 \\
 & [1101000000000000011100011100100001100000010100] \, \mathbf{w} & = 0.393 \times 47 \\
 & [0000000100001011010001000000100110100010100 1010] \, \mathbf{w} & = 0.273 \times 47 \\
 & [1101000000100001011000001110100010000000110100] \, \mathbf{w} & = 0.393 \times 47 \\
 & [0000000011000000010101010000000010110011101 0010] \, \mathbf{w} & = 0.133 \times 47 \\
 & [1111111100101000100000011111000010010000100100] \, \mathbf{w} & = 0.533 \times 47 \\
 & [1000000001010110010110100000001000000011101 0011] \, \mathbf{w} & = 0.273 \times 47 \\
 & [0111011110101001100000010001100100011000010 0000] \, \mathbf{w} & = 0.393 \times 47 \\
 & [0000001001010100010000100001000000001111000 0110] \, \mathbf{w} & = 0.273 \times 47 \\
 & [0011000110101001000101011100000001110000101 0000] \, \mathbf{w} & = 0.393 \times 47 \\
 & [0011000100100010000001001000110011010000110 0000] \, \mathbf{w} & = 0.333 \times 47 \\
 & [1100111011000001010000110101000100101000001 1001] \, \mathbf{w} & = 0.333 \times 47 \\
 & [0010000100101010000101000000111011010000010 0010] \, \mathbf{w} & = 0.333 \times 47 \\
 & [1100110001010000111000010010000100100001101 1101] \, \mathbf{w} & = 0.333 \times 47 \\
 & [0000000000100111000001000000111001010100000 0010] \, \mathbf{w} & = 0.273 \times 47 \\
 & [1101111011010000010000011011000000100010111 1101] \, \mathbf{w} & = 0.393 \times 47 \\
 & [0000000000010010100001100000111101010000000 0010] \, \mathbf{w} & = 0.263 \times 47 \\
 & [1111111010001001000000001011000000100110111 1001] \, \mathbf{w} & = 0.403 \times 47 \\
 & [0100000000010000100000110010011101010000100 0100] \, \mathbf{w} & = 0.333 \times 47 \\
 & [1001111010001000000000001001100010101110011 1000] \, \mathbf{w} & = 0.333 \times 47 \\
 & [0100000100010000010000100000010100010000000 0000] \, \mathbf{w} & = 0.333 \times 47 \\
 & [1010111010100111000101001101100001001111011 0000] \, \mathbf{w} & = 0.333 \times 47 \\
 & [0100110010001011100000000110101110000001000 0001] \, \mathbf{w} & \leq 0.333 \times 47 \\
 & [0110111111011011110001001110101111011111101 1111] \, \mathbf{w} & \leq 0.666 \times 47 \\
 & [0010001101010000010001001000000001011110101 1110] \, \mathbf{w} & \leq 0.333 \times 47 \\
 & [0001100000000111001000100100010001110001001 0000] \, \mathbf{w} & \leq 0.333 \times 47 \\
 & [0010001110111000110011010001000000001000000 0011] \, \mathbf{w} & \leq 0.334 \times 47 \\
 & [0011101110111111111011110101010001111001001 0011] \, \mathbf{w} & \leq 0.667 \times 47 \\
 & [0001000000000000001100001010100011000000110 0010] \, \mathbf{w} & \leq 0.333 \times 47 \\
 & [0110100101010010100001000001010100001011000 1100] \, \mathbf{w} & \leq 0.334 \times 47 \\
 & [0111100101010010101101001011110111001011110 1110] \, \mathbf{w} & \leq 0.667 \times 47 \\
 & [0000000000100111000001000000111011010100000 0010] \, \mathbf{w} & \leq 0.333 \times 47 \\
 & [0010000100001000101110100100000100001001010 0000] \, \mathbf{w} & \leq 0.334 \times 47 \\
 & [0010000100101111101111100100111111011101010 0010] \, \mathbf{w} & \leq 0.667 \times 47 \\
 & [1011111110111101010111101110110110110110111 1010111] \, \mathbf{w} & \leq 0.667 \times 47 \\
 & [0010000000011100000011100100110010000100100 0010] \, \mathbf{w} & \leq 0.334 \times 47 \\
 & [1001111110100001010100001010000100110011001 0101] \, \mathbf{w} & \leq 0.333 \times 47
\end{array}
$$

Figure 6. Alternate Representation of (24), (11), and Equations in Figure 5 as (20).

estimates without the forecasts to that made with the forecasts in Figure 1. There is a large shift, making all flows more likely to be exceeded.

Next, consider the annual maximum daily flow defined over the *water year*. Now, for example, the first value in Table 1, column 4, for water year 1949 (1 October 1948—30 September 1949) corresponds to the objective function of (24) and forecast values of Figure 5 for September 1948—August 1949 (to make spring snowmelt reflect the effect of the forecast). This leads to

the same equation set as obtained before in Figure 6, yielding the same weights. These weights are now applied to the water year data in column 4 of Table 1 by using (15)—(18) to make the distribution fit shown in Figure 2. The shift to increased exceedance frequency occurs for flows greater than 36000 cfs. Below this flow, there is actually a slight decrease in the exceedance frequency.

7. ENSO CONDITIONAL FORECAST EXAMPLE

As a second set of examples, the El Niño and La Niña conditional probabilities are used to bias storm frequency estimates. First, consider where these conditional probability estimates might come from. [ENSO-type conditioning has been applied elsewhere for statistical downscaling; see for example Katz and Parlange (1993, 1996).] The two phases of the El Niño – Southern Oscillation (ENSO) are the El Niño and La Niña events and refer to the oceanic and atmospheric circulation in and over the equatorial Pacific. It is recognized that weather in many parts of the world is related to the occurrence of El Niño and La Niña. The study of historical El Niño and La Niña events in Table 6 can yield event probabilities useful in hydrology or other derivative outlooks. A simple technique may be applied to derive probabilistic meteorology forecasts that consider the influence of El Niño, La Niña. That is, probabilities of various meteorological events can be estimated from the historical meteorological record *conditioned* on the occurrence of El Niño, La Niña, or the absence of both (Croley 2000a). Then, given that one of these three events is occurring at the time of a forecast, the appropriate set of conditional probabilities can be used as a probabilistic meteorological forecast.

The definition of the occurrence of these events is taken from Shabbar and Khandekar (1996). Strong to moderate ENSO years are defined as those in which the 5-month running Southern Oscillation Index (mean difference in sea-level pressure between Tahiti and Darwin) remained in the lower 25% (El Niño) or upper 25% (La Niña) of the distribution for 5 months or longer. This definition is consistent with that used by Rasmusson (1984), Ropelewski and Jones (1987), and Halpert and Ropelewski (1992). Table 6 contains the years of onset of strong or moderate El Niño and La Niña events, as given originally by Shabbar and Khandekar (1996) and corrected and extended by Shabbar et al. (1997).

By inspecting the historical meteorology record for those years of El Niño or La Niña in Table 6, one can estimate the probability of any event following an El Niño or La Niña with the event's relative frequency. For example, in the Great Lakes, there is much interest in the effects of ENSO on winter precipitation and air temperatures. Figure 7 presents selected relative frequencies of precipitation and air temperature over the Lake Erie basin (to be used over the Maumee River basin). Given that an El Niño or La Niña is occurring, the numbers in Figure 7 can be interpreted as forecast probabilities conditioned on the El Niño or La Niña occurrence.

The La Niña probabilities in Figure 7 are similar to the forecasts of Figure 5; those forecasts are predicated on a La Niña occurring. Therefore the right-most 12 equations in Figure 7 are used, in order, with the objective function of (24) to estimate a La Niña influence. Again, one can construct an equation set similar to (20), as at the top of Figure 8, by inspecting Tables 2—5 for values in (24), (11), and the right-side 12 equations in Figure 7. Optimization of the top equation

Table 6. El Niño and La Niña event onset years[a].

Year (1)	Event (2)	Year (3)	Event (4)	Year (5)	Event (6)	Year (7)	Event (8)
1900		1924	La Niña	1948		1972	El Niño
1901		1925	El Niño	1949		1973	La Niña
1902	El Niño	1926	El Niño	1950	La Niña	1974	
1903		1927		1951	El Niño	1975	La Niña
1904	La Niña	1928	La Niña	1952		1976	El Niño
1905	El Niño	1929	El Niño	1953	El Niño	1977	
1906		1930	El Niño	1954		1978	
1907		1931		1955	La Niña	1979	
1908		1932		1956	La Niña	1980	
1909	La Niña	1933		1957	El Niño	1981	
1910	La Niña	1934		1958	El Niño	1982	El Niño
1911	El Niño	1935		1959		1983	
1912	El Niño	1936		1960		1984	
1913		1937		1961		1985	
1914	El Niño	1938	La Niña	1962		1986	El Niño
1915		1939	El Niño	1963		1987	
1916	La Niña	1940		1964	La Niña	1988	La Niña
1917	La Niña	1941	El Niño	1965	El Niño	1989	
1918	El Niño	1942		1966		1990	
1919	El Niño	1943		1967		1991	El Niño
1920		1944		1968		1992	
1921		1945		1969	El Niño	1993	
1922		1946		1970	La Niña	1994	
1923		1947		1971	La Niña		

[a]After Shabbar and Khandekar (1996) and Shabbar et al. (1997).

set in Figure 8 matches the first 9 La Niña equations in Figure 7 to yield weights for estimating the La Niña climate-biased storm frequencies by using (15)—(18). These are for the annual maximum (calendar year) daily flow data in column 3 of Table 1 and for the annual maximum daily precipitation intensity data in column 2 of Table 1. These are shown in Figures 9 and 10, respectively, along with the unbiased storm frequency estimates. (Again, only parametric estimates are shown to simplify the presentation.)

The El Niño probabilities in Figure 7 appear more significant for air temperature than they do for precipitation. The objective in matching these forecasts is taken (arbitrarily here) as maximizing the probability that air temperature over the period November 1999—April 2000 will be in the upper third of its historical range (determined from 1961-1990).

$$\max \hat{P}\left[T_{Nov'99-Apr'00} > \hat{\tau}_{Nov-Apr,\,0.667} \right] \tag{27}$$

The left-most 12 equations in Figure 7 are used in order with the objective function of (27) to estimate an El Niño influence. Again, one can construct an equation set similar to (20), as at the

Maumee River Basin ENSO-Conditional Probability Estimates (as Forecasts)
SON 1999, DJF 1999, and MAM 2000 Air Temperature (T) & Precipitation (Q)
(Based on 1948-1995 data and 1961-1990 quantiles)

Conditional on El Niño	Conditional on La Niña
$\hat{P}\left[T_{SON'99} \le \hat{\tau}_{SON,0.333}\right] = 0.364$	$\hat{P}\left[T_{SON'99} \le \hat{\tau}_{SON,0.333}\right] = 0.111$
$\hat{P}\left[T_{SON'99} > \hat{\tau}_{SON,0.667}\right] = 0.273$	$\hat{P}\left[T_{SON'99} > \hat{\tau}_{SON,0.667}\right] = 0.444$
$\hat{P}\left[Q_{SON'99} \le \hat{\theta}_{SON,0.333}\right] = 0.273$	$\hat{P}\left[Q_{SON'99} \le \hat{\theta}_{SON,0.333}\right] = 0.444$
$\hat{P}\left[Q_{SON'99} > \hat{\theta}_{SON,0.667}\right] = 0.273$	$\hat{P}\left[Q_{SON'99} > \hat{\theta}_{SON,0.667}\right] = 0.444$
$\hat{P}\left[T_{DJF'99} \le \hat{\tau}_{DJF,0.333}\right] = 0.273$	$\hat{P}\left[T_{DJF'99} \le \hat{\tau}_{DJF,0.333}\right] = 0.000$
$\hat{P}\left[T_{DJF'99} > \hat{\tau}_{DJF,0.667}\right] = 0.636$	$\hat{P}\left[T_{DJF'99} > \hat{\tau}_{DJF,0.667}\right] = 0.444$
$\hat{P}\left[Q_{DJF'99} \le \hat{\theta}_{DJF,0.333}\right] = 0.636$	$\hat{P}\left[Q_{DJF'99} \le \hat{\theta}_{DJF,0.333}\right] = 0.222$
$\hat{P}\left[Q_{DJF'99} > \hat{\theta}_{DJF,0.667}\right] = 0.273$	$\hat{P}\left[Q_{DJF'99} > \hat{\theta}_{DJF,0.667}\right] = 0.444$
$\hat{P}\left[T_{MAM'00} \le \hat{\tau}_{MAM,0.333}\right] = 0.091$	$\hat{P}\left[T_{MAM'00} \le \hat{\tau}_{MAM,0.333}\right] = 0.556$
$\hat{P}\left[T_{MAM'00} > \hat{\tau}_{MAM,0.667}\right] = 0.364$	$\hat{P}\left[T_{MAM'00} > \hat{\tau}_{MAM,0.667}\right] = 0.111$
$\hat{P}\left[Q_{MAM'00} \le \hat{\theta}_{MAM,0.333}\right] = 0.273$	$\hat{P}\left[Q_{MAM'00} \le \hat{\theta}_{MAM,0.333}\right] = 0.222$
$\hat{P}\left[Q_{MAM'00} > \hat{\theta}_{MAM,0.667}\right] = 0.364$	$\hat{P}\left[Q_{MAM'00} > \hat{\theta}_{MAM,0.667}\right] = 0.778$

Figure 7. ENSO Event Conditional Probability Forecast Equations for Maumee River Basin.

bottom of Figure 8, by inspecting Tables 2—5 for values in (27), (11), and the left-side 12 equations in Figure 7. Optimization of the bottom of Figure 8 matches all 12 El Niño equations in Figure 7 to yield weights for estimating the El Niño storm frequencies in Figures 9 and 10.

Figure 9 shows that the effect of considering La Niña conditions, with the objective of maximizing higher precipitation probability, increases the probability for all flows to be exceeded. The effect of El Niño conditions, with the objective of maximizing higher temperature probability, increases the exceedance probability for flows below about 77000 cfs, but decreases it for flows above. In Figure 10, the effects on maximum precipitation intensity are more mixed. La Niña and the maximization of higher precipitation probability increase the exceedance probability for precipitation rates above about 3.5 mm/day but decrease it below. El Niño and the maximization of higher temperature probability decrease the exceedance probability for precipitation rates above about 2.7 mm/day and only slightly increase it above.

Even though one can exactly match meteorological forecasts, that does not mean that the resulting climate-biased storm frequencies contain no other errors. Sampling errors still exist and can

THE OBJECTIVE OF (24), (11), AND THE RIGHT-MOST 12 EQUATIONS (LA NIÑA) IN FIGURE 7:

$$\max \quad [1111000000100000001110001010000100100100110010 0]\ \mathbf{w} \quad \text{subject to}$$

$$\begin{aligned}
&[1111111111111111111111111111111111111111111111]\ \mathbf{w} = 47\\
&[0001000000000000001101001010100011000000110001 0]\ \mathbf{w} = 0.111 \times 47\\
&[1000011010101101010000110100001000010100001000 1]\ \mathbf{w} = 0.444 \times 47\\
&[0100110010001011100000000110101110000001000000 1]\ \mathbf{w} = 0.444 \times 47\\
&[0010001101010000010001001000000001011110101111 0]\ \mathbf{w} = 0.444 \times 47\\
&[0000000000100111000001000000111001010100000001 0]\ \mathbf{w} = 0.000 \times 47\\
&[1101111011010000010000011011000000100010111110 1]\ \mathbf{w} = 0.444 \times 47\\
&[0000000100001011010001000000100110100010100101 0]\ \mathbf{w} = 0.222 \times 47\\
&[1101000000100001011000001110100010000000110100]\ \mathbf{w} = 0.444 \times 47\\
&[0100000100010000010000100000010100010000000000]\ \mathbf{w} = 0.556 \times 47\\
&[1010111010100111000101001101100001001111011000 0]\ \mathbf{w} = 0.111 \times 47\\
&[0000001001010100010000100001000000001111000011 0]\ \mathbf{w} = 0.222 \times 47\\
&[0011000110101001000101011100000001110000101000 0]\ \mathbf{w} = 0.778 \times 47
\end{aligned}$$

THE OBJECTIVE OF (27), (11), AND THE LEFT-MOST 12 EQUATIONS (EL NIÑO) IN FIGURE 7:

$$\max \quad [1101111011000000011000001101000000101010011100 1]\ \mathbf{w} \quad \text{subject to}$$

$$\begin{aligned}
&[1111111111111111111111111111111111111111111111]\ \mathbf{w} = 47\\
&[0001000000000000001101001010100011000000110001 0]\ \mathbf{w} = 0.364 \times 47\\
&[1000011010101101010000110100001000010100001000 1]\ \mathbf{w} = 0.273 \times 47\\
&[0100110010001011100000000110101110000001000000 1]\ \mathbf{w} = 0.273 \times 47\\
&[0010001101010000010001001000000001011110101111 0]\ \mathbf{w} = 0.273 \times 47\\
&[0000000000100111000001000000111001010100000001 0]\ \mathbf{w} = 0.273 \times 47\\
&[1101111011010000010000011011000000100010111110 1]\ \mathbf{w} = 0.636 \times 47\\
&[0000000100001011010001000000100110100010100101 0]\ \mathbf{w} = 0.636 \times 47\\
&[1101000000100001011000001110100010000000110100]\ \mathbf{w} = 0.273 \times 47\\
&[0100000100010000010000100000010100010000000000]\ \mathbf{w} = 0.091 \times 47\\
&[1010111010100111000101001101100001001111011000 0]\ \mathbf{w} = 0.364 \times 47\\
&[0000001001010100010000100001000000001111000011 0]\ \mathbf{w} = 0.273 \times 47\\
&[0011000110101001000101011100000001110000101000 0]\ \mathbf{w} = 0.364 \times 47
\end{aligned}$$

Figure 8. Alternate Equations Sets for La Niña and El Niño Examples as in (20).

be pronounced if many meteorological time series segments are weighted by zero and effectively eliminated from the sample. This happened in the ENSO conditioned examples. Only 11 La Niña example weights were non-zero (out of 47) and only 19 El Niño weights were non-zero.

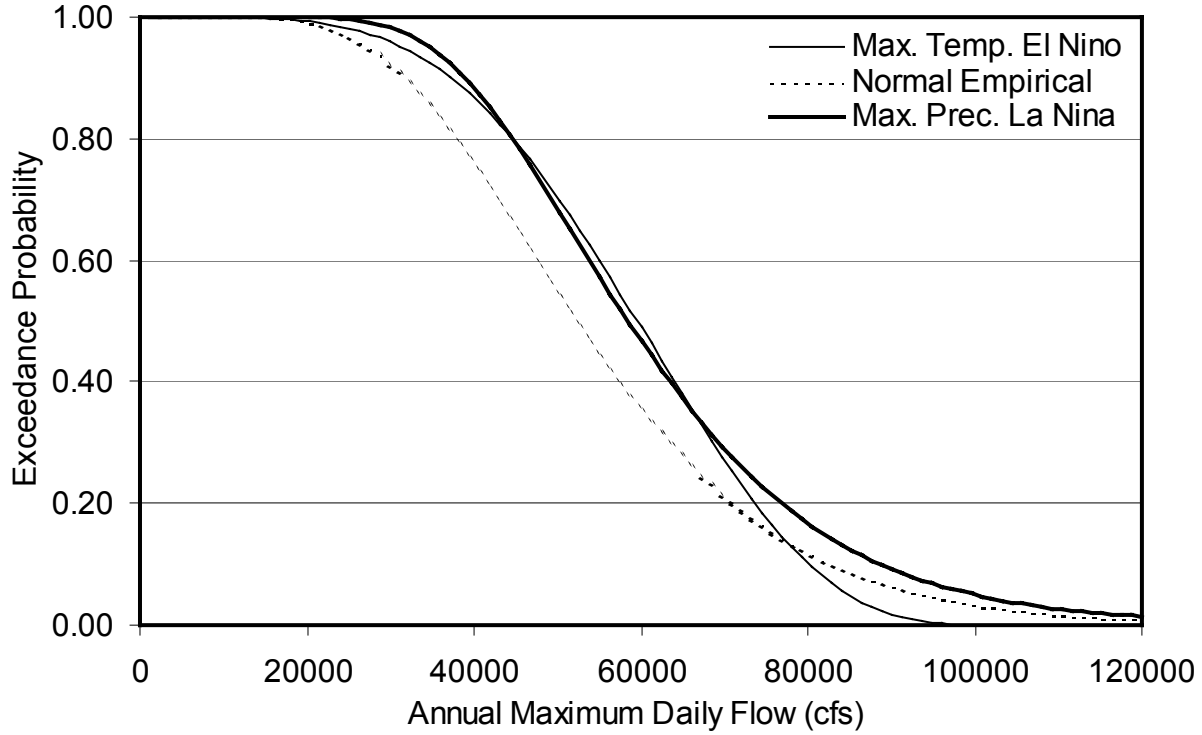

Figure 9. ENSO Annual Maximum (Calendar Year) Daily Maumee River Flow Exceedance.

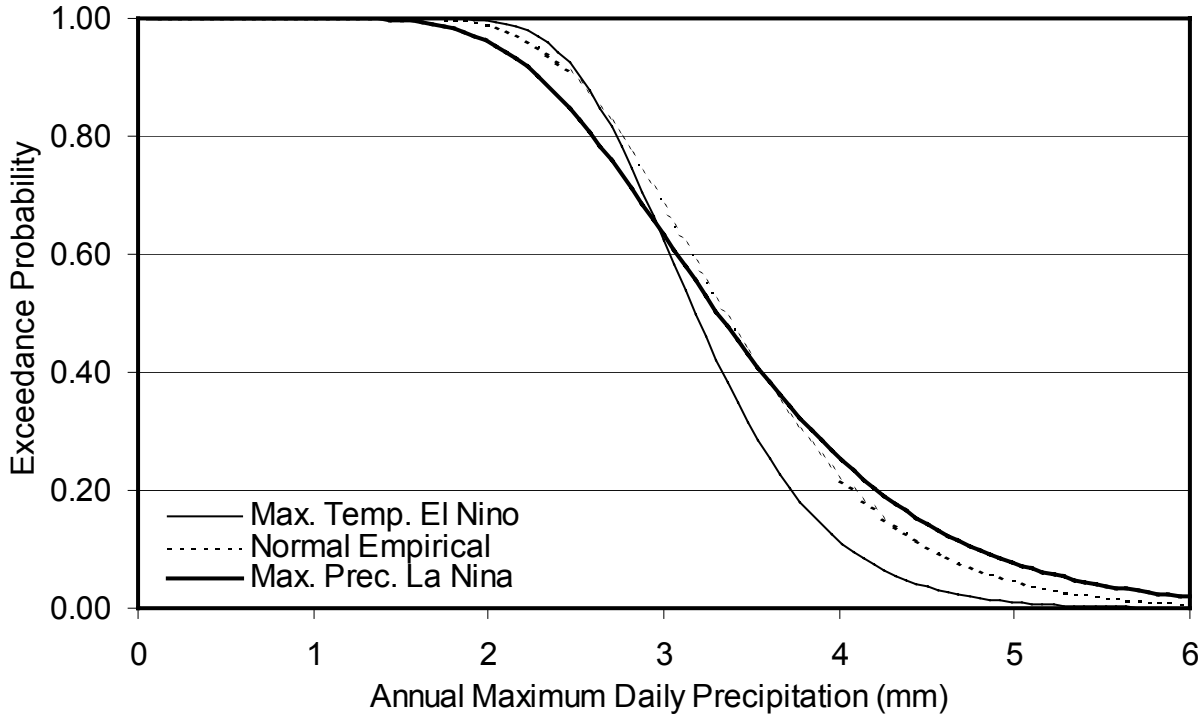

Figure 10 ENSO Annual Maximum Daily Maumee River Basin Precipitation Exceedance.

8. MULTIPLE SOLUTIONS

In the optimization of (20), all expressions are *linear*, including the objective function [first line in (20)]. This allows a linear programming optimization technique to be used as compared to earlier formulations (Croley 1996, 1997b). Those used the minimization of the sum of squared differences of each weight with unity, $\sum(w_i - 1)^2$, and employed classical differential calculus solutions for zero slope of the Lagrangian. The linear formulation proves superior in its ability to include alternate objectives (expressed as maximization of selected event probabilities). Also, the formulation of (20) allows non-negativity constraints on the weights to be *explicitly* included. This means that *all* solutions can be searched. The earlier formulations of Croley (1996, 1997b) lacked explicit inclusion of non-negativity constraints for the weights. There, optimum solutions were considered and discarded (along with lowest-priority constraints) if non-negativity constraints were unsatisfied. But that also discarded the many other possibilities that, while not optimum, might satisfy all constraints.

There is a trade-off however. Multiple optima solutions are now a possibility that did not exist before. In the search algorithms employed in the linear programming solutions, these multiple optima can be detected (that is, the existence of more than a single optimum can be discerned) but the systematic exploration of them can be extensive. Croley (2000a,b) describes this further. Here, it is sufficient to note that, in the examples of Figures 1 and 2, the optimum was unique. In the examples of Figures 9 and 10, the optima were not unique. The optimization for the La Niña examples yielded 8 solution points in the systematic search with the Simplex method. Four of these were unique but discovered twice. The optimization for the El Niño examples yielded over 5000 solution points (the limit on the search); 36 were unique. In both of these cases, the average of the found unique optima were used for weighting (biasing) the sample in estimating storm frequencies.

9. SUMMARY AND OBSERVATIONS

The methodology described herein allows one to recognize changing climate in the estimation of storm frequencies, removing one of the worst assumptions associated with this, which is that future probabilities are the same as the past. Existing forecasts of meteorology probabilities can be used to bias storm frequency estimates for a changing climate. The methodology is adapted from earlier work that uses forecasts of meteorology probabilities to derive forecasts of consequent hydrology probabilities in an operational hydrology approach. The linear objective function used here enables incorporation of an event probability into the objective, use of existing optimization techniques, and direct inclusion of non-negativity constraints.

The examples presented here are provided to supplement and further illustrate the methodology described elsewhere (Croley 2000a,b). These examples may be more representative of storm frequency estimation in an *operational* setting rather than in a *design* setting. Climate-biased storm frequencies were estimated by *preserving* meteorology forecasts. These conditions are current and are not generally regarded as applying over a very long time into the future. The resulting biased storm frequencies can only be considered applicable over the same time period as the meteorology forecasts or other event probabilities used to condition them. The examples given here

applied over the next several months, appropriate for use in an operational setting. If probabilities can be defined (estimated) corresponding to climate shifts expected from the present forward, then the resulting biased storm frequencies could be used in a design setting.

Complete software, in the form of an easy-to-use interactive *Windows ™* graphical user interface, and worked examples are available free of charge over the World Wide Web. The software, examples, and tutorial materials may be acquired in a self-installing file by visiting the web site entitled: http://www.glerl.noaa.gov/wr/OutlookWeights.html and downloading.

10. REFERENCES

Chow, V. T., 1964. *Handbook of Applied Hydrology*. McGraw-Hill, New York, 8-29.

Croley, T.E., II, 1996. Using NOAA's New Climate Outlooks In Operational Hydrology. *Journal of Hydrologic Engineering*, ASCE, **1**(3):93-102.

Croley, T.E., II, 1997a. Water resource predictions from meteorological probability forecasts. *Proceedings, Sustainability of water resources under increasing uncertainty (Proc. Rabat Symp.)*, D. Rosbjerg et al., ed., IAHS Publication No. 240, IAHS Press, Wallingford, U.K., 301-309.

Croley, T.E., II, 1997b. Mixing Probabilistic Meteorology Outlooks In Operational Hydrology. *Journal of Hydrologic Engineering*, ASCE, **2**(4):161-168.

Croley, T. E., II, 2000a. *Using Meteorology Probability Forecasts In Operational Hydrology*. ASCE Press, American Society of Civil Engineers, Reston, Virginia, 214 pp

Croley, T. E., II, 2000b. Climate-Biased Storm-Frequency Estimation. *Journal of Hydrologic Engineering*, ASCE, (in review).

Halpert, M. S., and C. F. Ropelewski, 1992. Surface temperature patterns associated with the Southern Oscillation. *Journal of Climate* **5**:577–93.

Hillier, F. S., and G. J. Lieberman, 1969. *Introduction to Operations Research*. Chapter 5: Linear Programming, Holden-Day, San Francisco, 127-171.

Katz, R. W., and M. B. Parlange, 1993. Effects of an index of atmospheric circulation on stochastic properties of precipitation. *Water Resources Research* **29**:2335-2344.

Katz, R. W., and M. B. Parlange, 1996. Mixtures of stochastic processes: application to statistical downscaling. *Climate Research* **7**:185-193.

Koutrouvelis, I. A., and G. C. Canavos, 1999. Estimation In The Pearson Type 3 Distribution. *Water Resource Research*, AGU, **35**(9):2693-2704.

Rasmusson, E. M., 1984. El Niño: The ocean/atmosphere connection. *Oceanus* **27**(2):5–12.

Ropelewski, C. F., and P. D. Jones, 1987. An extension of the Tahiti-Darwin Southern Oscillation index. *Monthly Weather Review* **115**:2161–65.

Shabbar, A., B. Bonsal, and M. Khandekar, 1997. Canadian precipitation patterns associated with the Southern Oscillation. *Journal of Climate* **10**:3016–27.

Shabbar, A., and M. Khandekar, 1996. The impact of El Niño–Southern Oscillation on the temperature field over Canada. *Atmosphere Ocean* **34**(2):401–16.

U.S. Water Resources Council, 1967. A Uniform Technique For Determining Flood-Flow Frequency. *Bulletin 15*, Hydrology Committee, Washington, DC, 1967.